Spallation studies at GSI

L. Giot[1*], P. Napolitani[2], M. F. Ordonez[3], D. Henzlova[1,11], L. Audouin[2], J. Benlliure[3], A. Boudard[4], E. Casajeros[3], J. E. Ducret[4], T. Enqvist[5], A. Heinz[6], V. Henzl[1,11], A. Junghans[7], B. Jurado[8], A. Kelić[1], A. Krasa[11], T. Kurtukian[3], S. Leray[4], J. Pereira[3], R. Pleskač[1], F. Rejmund[9], M. V. Ricciardi[1], C. Schmitt[10], C. Stephan[2], K.-H. Schmidt[1], L. Tassan-Got[2], C. Villagrasa[4], C. Volant[4], A. Wagner[7] and O. Yordanov[1]

CHARMS: Collaboration for High-Accuracy Experiments on nuclear Reaction Mechanisms with the magnetic spectrometers involving: (***http://www-w2k.gsi.de/charms/***)
1) GSI, Planckstraße 1, 64291 Darmstadt, Germany
2) IPN Orsay, IN2P3, 91406 Orsay, France
3) University of Santiago de Compostela, 15706 Santiago de Compostela, Spain
4) DAPNIA/SPhN CEA/Saclay, 91191 Gif-sur-Yvette, France
5) CUPP Project, P. O. Box 22, 86801, Pyhäsalmi, Finland
6) Wright Nuclear Structure Laboratory, Yale University, New Heaven, CT 06520, USA
7) Forschungenszentrum Rossendorf, 01314 Dresden, Germany
8) CENBG, IN2P3, 33175 Gradignan, France
9) GANIL, Bd H. Becquerel, BP 5027, 14000 Caen, France
10) IPNL, 43 Bd du 11 Novembre, 69622 Villeurbanne, France
11) Nuclear Physics Institute, 25068 Rez, Czech Republic.

Abstract: An extended experimental and theoretical campaign dedicated to the studies of spallation reactions in inverse kinematics has been performed at GSI, Darmstadt. This research program on spallation reactions is based on an innovative experimental approach, which exploits the unique installations of GSI: the accelerator complex provides heavy-ion beams at relativistic energies, while a high-resolution magnetic spectrometer is used to identify the reaction products in-flight in mass and atomic number and to determine their kinematical properties. In this paper, we report the results obtained in this program on the spallation of ^{136}Xe on protons at 500 *A* MeV.

INTRODUCTION

The complete understanding and modelling of proton-induced spallation reactions is a major goal both for technical applications as well as for fundamental research. Spallation reactions are mandatory for developing intense neutrons sources needed for accelerator-driven systems (ADS) for incineration of nuclear waste [Bowm92, Rubb93, Rubb95], material physics and biology [Ess00] and also to produce high intensity radioactive beams [Ridi00, Euri04]. In addition, spallation reactions are a subject of interest in astrophysics to understand the origin of cosmic rays and their reactions with the hydrogen and helium nuclei in the interstellar medium [Arno61, Ross33]. All these perspectives have triggered a long-range research program at GSI, devoted to reach a full comprehension of the proton and deuteron-induced spallation reactions by measurements of evaporation residues and fission fragments.

The experimental investigations on spallation reactions are usually performed in direct kinematics by bombarding various target materials with protons or deuterons of the energy of interest and by analysing the produced species after irradiation, e.g. by their radioactive decay or by mass spectrometry. These direct methods can only give a limited insight into the reaction mechanism, because short-lived products, which form the dominant production in most cases, cannot be observed due to the time delay between the irradiation and the measurement. Information on the reaction kinematics is also not easily accessible. On the contrary, in these experiments the excitation functions restricted to a few residues can be easily measured [Glor01, Mich97]. An alternative experimental approach, based on the inverse-kinematics, was developed at GSI to overcome most of the limitations of the direct method. The short times of flight (below 300 ns) of the heavy ions at relativistic energies coupled to the use of the FRS

* l.giot@gsi.de

spectrometer at GSI allow the detection of the primary products before β decay and give also access to their kinematical properties. Moreover, the reconstruction of the full velocity distribution allows for disentangling reaction products formed in fragmentation and fission reactions due to their different kinematic properties. For nuclides produced by fission, only those emitted either in forward or in backward direction with respect to the primary beam can be observed in a given setting of the FRS because the angular acceptance is too small for sideward-emitted fragments [Benl02].

Large sets of new experimental data with unprecedented quality have been accumulated in experiments in inverse kinematics at GSI during the HINDAS project [Hind]. About thousand nuclides per system were detected, identified unambiguously and analysed with a systematical incertitude in the order of 10% to 15% in most cases. The production cross sections of spallation reactions have been investigated for the following systems: ^{197}Au+p at 800 *A* MeV [Benl01, Rejm01], ^{208}Pb+p at 0.5 and 1 *A* GeV, [Fern05, Audo06, Wlaz00, Enqv01], ^{208}Pb+d at 1 *A* GeV [Enqv02], ^{238}U+p at 1 *A* GeV [Bern03, Taie03, Armb04, Ricc06], ^{238}U+d at 1 *A* GeV [Casa06, Pere06], ^{56}Fe+p in the range of 0.3-1.5 *A* GeV [Villa03, Napo04]. While the nuclear reactions occurring in a conventional fission reactor are limited to the energy range of fission neutrons below a few MeV, the nuclear reactions occurring in an accelerator-driven system, consisting of a sub-critical reactor and a neutron source driven by 1 GeV protons, extend to energies up to the primary proton energy. In addition to the detailed understanding of the neutronics and the complex transport phenomena of light particles, the production of heavy residues by proton- and neutron-induced fragmentation and fission reactions needs to be known for the design of such a system. This has decisive consequences for the shielding and the activation of the installation, the radiation damages of construction materials and the chemical properties of the spallation target. In contrast to the situation in conventional fission reactors, where all relevant nuclear data could be measured, the large range of energy and the variety of target materials involved in an accelerator-driven system demands for a different strategy. Only a limited number of selected key reactions can be studied in full detail and serve to benchmark, improve and develop nuclear-reaction codes, which are then used to calculate the reactions occurring in the accelerator-driven system in their full variety.

The study of the spallation of ^{136}Xe on protons is a step ahead in the extension of experimental data obtained at GSI and it will provide decisive information on the energy dependence of the spallation process. The understanding of the energy dependence of the spallation process is very important due to the energy loss of the proton beam in the spallation neutron source and due to the importance of secondary reactions initiated by particles emitted in the primary reactions. Furthermore, projects like MYRRHA [Myrr01] and MEGAPIE [Mega04] will use protons beams respectively of 360 MeV and 590 MeV to demonstrate the different components of ADS. For the light projectiles, the spallation of ^{56}Fe on protons at different energies between 0.3 *A* GeV and 1.5 *A* GeV was performed at GSI and in the case of heavy projectiles, the production cross sections were obtained for the reactions ^{208}Pb+p at 500 *A* MeV and 1 *A* GeV [Villa03, Audo06, Timo01]. To complete this study on the energy dependence of the spallation process and to fill the gap for the projectiles between ^{56}Fe and ^{208}Pb, the spallation reactions of ^{136}Xe on protons at 500 and 1000 *A* MeV were performed at GSI [Giot06, Napo06]. It is an ideal experimental case because this system allows performing measurements at the beam energy of 500 *A* MeV, without any ambiguities due to multiple ionic charge states in the nuclide identification of the evaporation products. The new data will help to develop improved models with better predictive power for spallation reactions involving nuclei spanning a wide mass range. In this paper, we will describe the experimental technique and the preliminary results obtained for the spallation of ^{136}Xe on protons at 500 *A* MeV.

EXPERIMENTAL TECHNIQUE

The experimental method and the analysis procedure have been developed and applied in the previous spallation experiments quoted above. The dedicated experimental set up is shown in Fig. 1. The heavy-ion synchrotron SIS at GSI, Darmstadt, delivers a ^{136}Xe primary beam at 500 *A* MeV. The primary-beam intensity, up to 4 10^7 particles/spill was continuously monitored by a beam monitor SEETRAM based on secondary-electrons emission [Jura02]. The proton target was composed of 87.3 mg/cm^2 [Rejm01, Enqv01] liquid hydrogen enclosed between thin titanium foils of a total thickness of 36 mg/cm^2 [Ches97, Rejm01]. In order to subtract the contribution from the target windows and also from other layers in the beam line to the measured reaction rate, measurements were repeated with the empty target container. The dead-time of the data acquisition, typically in the order of 25 % was continuously monitored. Heavy residues produced in the target were all strongly forward focused due to the high velocity of the incoming beam and the inverse kinematics. They were identified using the Fragment Separator (FRS) [Geis92] and the associated detector equipment.

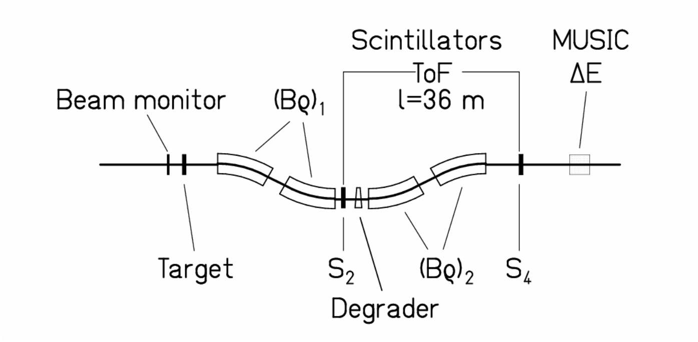

Fig. 1. Schematic view of the experimental setup.

The FRS is a two-stage magnetic spectrometer with a dispersive intermediate image plane (S_2) and an achromatic final image plane (S_4), with a momentum acceptance of ± 1.5% and an angular acceptance of about 15 mrad around the beam axis. Two position-sensitive plastic scintillators placed at S_2 and S_4, respectively, provided the magnetic-rigidity ($B\rho$) and time-of-flight measurements, which allowed determining the mass-over-charge ratio A/Z of the particles.

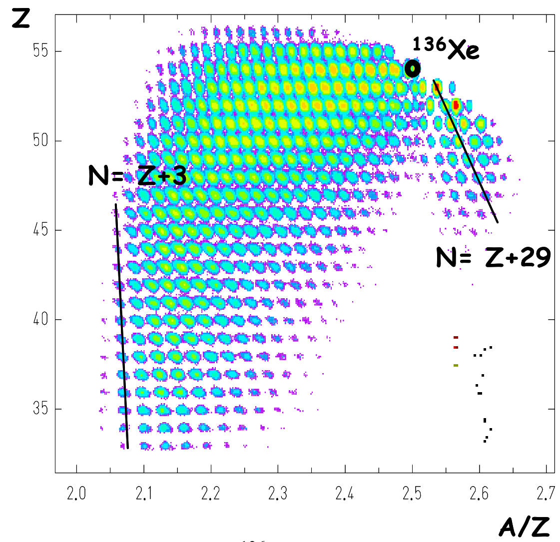

Fig. 2. Identification pattern of the measured data for the ^{136}Xe + p at 500 *A* MeV. The z-axis, i.e. the number of counts, is given on a logarithmic scale and is not normalized for each magnetic setting to the beam dose. The plot collects the counts from the hydrogen target, including the contribution from the titanium windows of the container and also other layers in the beam line.

The nuclear charge of the elements was deduced from the energy loss in two ionisation chambers (MUSIC) with a resolution $\Delta Z \sim 0.4$ [Pfüt94]. The energy-loss signal was corrected for the velocity dependence of the ion and for the recombination losses. The charge calibration was obtained from the projectile charge. Combining the nuclear-charge information with the mass-over-charge ratio, a complete isotopic identification was performed as shown on Fig. 2. and a mass resolution $A/\Delta A$ of 400 was achieved. For an unambiguous isotopic identification of the reaction products, the analysis was restricted to ions, which passed both stages of the fragment separator fully stripped. In order to avoid losses due to the limited momentum acceptance of the FRS, measurements with different values of the magnetic rigidity $B\rho$ were combined. The velocity v of the identified fragment was determined from the magnetic rigidity $B\rho$ at S_2 according to the equation

$$\beta\gamma\ \mathrm{c} = B\rho \frac{\mathrm{e}Z}{M} \tag{1}$$

where M is the mass of the nucleus, $\beta = v/\mathrm{c}$ and $\gamma = 1/\sqrt{1-\beta^2}$. The velocity was transformed into the reference frame of the beam in the middle of the target by Lorentz transformation, taking into account the appropriate energy losses in the corresponding part of the target. The relative uncertainty in the velocity was about $5\cdot10^{-4}$. The integral of the velocity distributions normalised to the beam intensity gives access to the yield of nuclei produced. The production cross sections were obtained from the measured yields knowing the target thickness and the angular acceptance of the FRS [Benl02]. For all the residues we measured, with a mass number above 70, the angular transmission was estimated to be between 70% for the lightest nuclei and 100% for the heaviest nuclei with an accuracy within 5%. The losses in counting rate due to the fraction of incompletely stripped ions, to the secondary reactions in the layers of matter in the beam line and to the dead-time of the data acquisition were corrected for. The beam attenuation in the target was also taken into account. The production cross sections obtained in the reaction ^{136}Xe + ^{1}H at 500 MeV per nucleon will be discussed in the next section.

RESULTS

Measured production cross sections

The measured cross sections of the isotopes of the elements between $Z = 33$ and $Z = 54$ produced in the ^{136}Xe + ^{1}H spallation reaction at 500 *A* MeV are presented on the Fig. 3. (left) as a cluster plot on the chart of nuclides. The evaporation residues below Z=33 could not be measured due to a lack of beam time. The single and double charge-pickup channels were observed (isotopes of elements $Z = 55, 56$). The charge pickup reactions proceed either through a quasi elastic collision between a proton and a neutron of the target and projectiles nuclei, respectively, where the proton replaces the neutron inside the projectile-like fragment, or through the excitation of a projectile (or target) nucleon into the Δ(1232) resonance state and its subsequent decay [Gaar91]. For comparison, Fig. 3. (right) shows the production cross sections of the nuclei measured in the spallation reaction ^{136}Xe + ^{1}H performed at higher energy (1 *A* GeV) with the same experimental setup [Napo06].

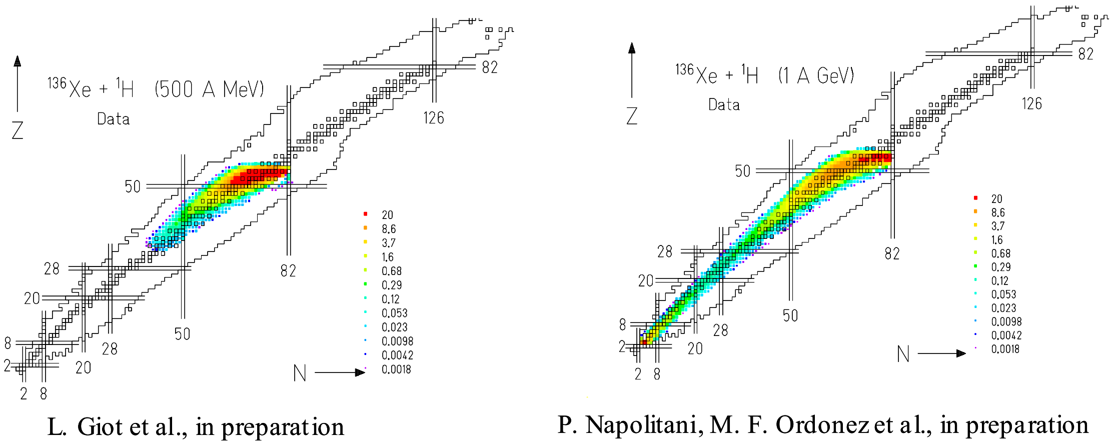

Fig. 3. Residual nuclide cross sections measured in the spallation reaction of ^{136}Xe on protons at 500 *A* MeV (left, preliminary data) and at 1 *A* GeV (right) shown on a chart of the nuclides. Nuclei with atomic number below 33 were not covered by the experiment at 500 *A* MeV.

The production cross sections of the evaporation residues close to the projectile are higher in the spallation reaction at 500 *A* MeV than at 1 *A* GeV, as expected. When the beam energy is increased from 500 *A* MeV to 1 *A* GeV, the total reaction cross section σ_R increases by less than 10% according to

Karol using a Glauber's approach [Karo75]. The total reaction cross section calculated with the Karol's formula at 1 *A* GeV (σ_R = 1353 mb) is in good agreement with the measured value (σ_R = 1393 ± 12 mb). In the case of the reaction at 1 *A* GeV, a mean excitation energy of 140 MeV is introduced instead of a mean excitation energy of 90 MeV for the reaction at 500 *A* MeV [Duar06]. The higher excitation energy compared to the reaction at 500 *A* MeV has the net effect that more nuclei are produced with a lower cross section for those close to the projectile. This study of the energy dependence of the spallation reaction will be completed by others experiments already under analysis, i.e. the spallation of ^{136}Xe on protons at 200 *A* MeV and the spallation of ^{136}Xe on deuterons at 500 *A* MeV.

Comparison with model calculations

Spallation reactions are understood in terms of a two steps process, as proposed by Serber [Serb47]. The first stage is usually modelled by individual nucleon-nucleon collisions with intra-nuclear-cascade codes, which ends with the rapid formation of a thermalised excited nuclear system. Then, the excited pre-fragment de-excites by emitting gamma-rays, nucleons, clusters and/or fission and this second stage is described by a statistical model of nuclear reactions. Here, we will compare our experimental results with two different intranuclear-cascade models, namely ISABEL of Yariv and Fraenkel [Yari81] and the Liège code of Cugnon (INCL4) [Cugn97, Boud02], followed by the same evaporation model ABLA developed at GSI [Gaim91, Jung98]. In Fig. 4., we show a comparison between the experimental isotopic cross sections for Z=53, 54 for the reaction ^{136}Xe + ^{1}H at 500 *A* MeV and the results from the codes INCL4+ABLA (blue line) and ISABEL+ABLA (green line). It can be seen in these calculations that the isotopic cross sections of the nuclei close to the projectile are better reproduces with a INCL4+ABLA combination. More detailed calculations will be undertaken in a near future on the charge and mass distributions of the evaporation residues. For example, we will study the influence of the de-excitation stage by varying the evaporation model, taking either ABLA, GEMINI [Char98] or the GEM code [Furi00], an updated version of code developed by Dresner et al.

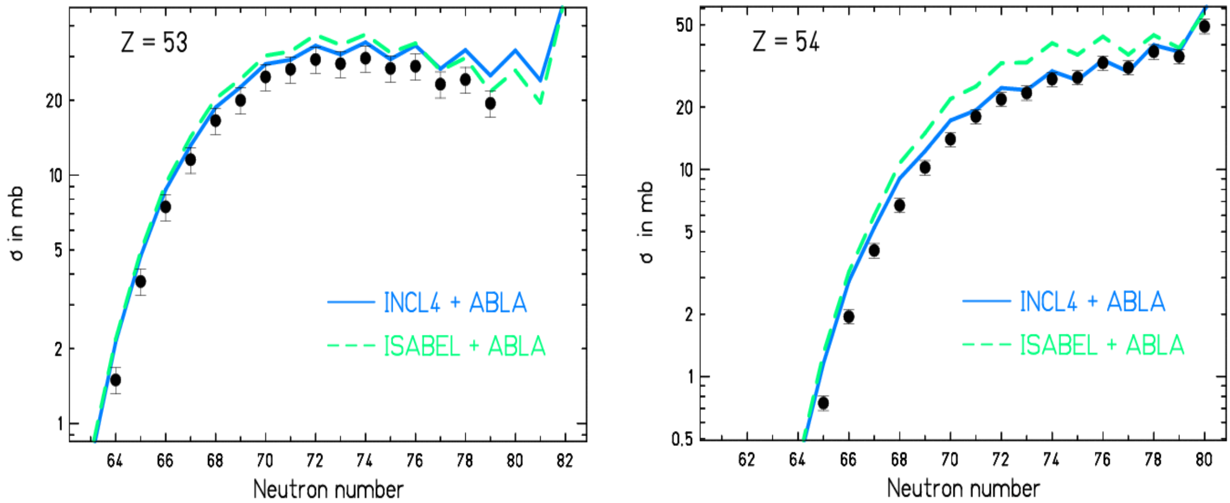

Fig. 4. Isotopic cross sections (preliminary data) for Z=53, 54 measured in the reaction of ^{136}Xe+^{1}H at 500 *A* MeV compared with INCL4+ABLA and the ISABEL+ABLA codes.

Another interesting feature is the even-odd staggering observed in the production cross sections for Z=53, 54. A similar effect was already observed for the heaviest residues in other spallation experiments in GSI [Napo06, Henz06]. It is known that the pairing interaction vanishes for excitation energies above 10 MeV. This even odd effect was reproduced by the ABLA code, as shown in Fig. 4., by following the idea developed by Ricciardi et al. for the light residues in the case of the fragmentation reaction ^{238}U + Ti at 1 *A* GeV that the structural effects are restored in the end products when the nucleus cool down and goes from the liquid to the superfluid phase [Ricci04]. Further investigations will be undertaken to study the competition between the influence of the angular momentum and of the de-excitation by gamma emission on the restoration of the even-odd effects close to the projectile.

CONCLUSIONS

An experimental and theoretical campaign dedicated to the study of the spallation reaction was undertaken at GSI. The measured production cross sections are of highest interest for the design of accelerator-driven systems and the systems investigated provide stringent constraints to nuclear-reaction codes. The comparison of the production of residual nuclei in the spallation reaction of ^{136}Xe induced by protons at different energies show the influence of a higher excitation energy, especially the decrease of $\sigma_{production}$ of the nuclei close to the projectile. Additionally, even-odd effects were observed in the isotopic distribution of the production cross sections of the heavy residues and these production cross sections were up to now better reproduced with a combination of the INCL4 intra-nuclear cascade and the statistical code ABLA.

Acknowledgements
The support provided during the experiment by K.H. Behr, A. Brünle and K. Burkard is gratefully acknowledged. We are thankful to the group of P. Chesny who built the liquid hydrogen target. This work was financially supported by the FP6 European Community Programme (Contract No FI6W-516352).

References
[Armb04] P. Armbruster et al., Phys. Rev. Lett. 93, 212701 (2004).
[Arno61] J. R. Arnold et al., J. Geophys. Res. 66 3519 (1961).
[Audo06] L. Audouin, Nucl. Phys. A768, 1 (2006).
[Benl01] J. Benlliure et al., Nucl. Phys. A683, 513 (2001).
[Benl02] J. Benlliure et al., Nucl. Instr. Meth. A478, 493 (2002).
[Bern03] M. Bernas et al., Nucl. Phys. A725, 213 (2003).
[Boud02] A. Boudard et al., Phys. Rev. C 66, 044615 (2002).
[Bowm92] C. D. Bowman et al., Nucl. Instr. Meth. A320, 336 (1992).
[Casa06] E. Casajeros et al., accepted in Phys. Rev C.
[Char98] R. Charity, Phys. Rev. C 58, 1073 (1998).
[Ches97] P. Chesny et al., GSI –Annual Report 97-1, 190 (1997).
[Cugn97]J. Cugnon et al., Nucl. Phys. A620, 475 (1997).
[Duar06] H. Duarte et al., accepted in Phys. Rev. C.
[Enqv01] T. Enqvist et al., Nucl. Phys. A686, 481 (2001).
[Enqv02] T. Enqvist et al., Nucl. Phys. A703, 435 (2002).
[Ess00] The ESS project, vol. II., New science and technology for the 21st century, ISBN 3-89336-302-5, available at http://neutron.neutron-eu.net/n\ess/.
[Euri04] The EURISOL report, available at www.ganil.fr/eurisol/Final-Report.html.
[Fern05] B. Fernandez-Dominguez et al., Nucl. Phys. A747, 227 (2005).
[Furi00] S. Fuhirata, Nucl. Instr. and Meth. B 171, 251 (2000).
[Gaar91] C .Gaarde, Annu. Rev. Nucl. Part. Sci. 41 (1991) 187.
[Gaim91] J-J Gaimard and K.-H. Schmidt, Nucl. Phys. A531(1991) 709.
[Geis92] H. Geissel et al., Nucl. Instr. Meth. B70, 286 (1992).
[Giot06] L. Giot et al., in preparation.
[Glor01] M. Gloris et al., Nucl. Instr. Meth. A463, 593 (2001).
[Henz06] D. Henzlova, Thesis of University of Prague, 2006.
[Hind] http://www.fynu.ucl.ac.be/collaboration/hindas/
[Jung98] A. R. Junghans et al., Nucl. Phys. A629, 635 (1998).
[Jura02] B. Jurado et al., Nucl. Instr. Meth. A483, 603 (2002).
[Karo75] P. J. Karol, Phys. Rev. C11, 1203 (1975).
[Mega04] F. Groeschel et al., Journal of Nucl. Mat. 335, 156 (2004).

[Myrr01] H. Ait Abderrahim et al., Nucl. Instr. Methods A 463, 487 (2001).
[Napo04] P. Napolitani et al., Phys. Rev. C 70, 054607 (2004).
[Napo06] P. Napolitani et al., in preparation.
[Peir06] J. Pereira et al., submitted to Phys. Rev. C.
[Pfüt94] M. Pfützner et al., Nucl. Instr. Meth B86, 213 (1994).
[Rejm01] F. Rejmund et al., Nucl. Phys. A683, 540 (2001).
[Ricci04] M. V. Ricciardi et al., Nucl. Phys. A733, 299 (2004).
[Ricci06] M. V. Ricciardi et al., Phys. Rev. C 73, 014607 (2006).
[Ridi00] D. Ridikas, W. Mittig, N. Alamanos, Internal CEA report, 2000, Dapnia-SphN-200-59.
[Ross33] G. Rossi, Z. Phys. 82, 151 (1933).
[Rubb93] C. Rubbia et al., Report CERN/AT/93-47/(ET), 1993.
[Rubb95] C. Rubbia et al., Report CERN/AT/95-44/(ET), 1995.
[Serb47] R. Serber, Phys. Rev. C 72, 1114 (1947).
[Taie03] J. Taïeb et al., Nucl. Phys. A724, 413 (2003).
[Villa03] C. Villagrasa, PhD thesis (2003), University of Paris XI, France.
[Wlaz00] W. Wlazlo et al., Phys. Rev. Lett 84, 5736 (2000).
[Yari81] Y. Yariv and Z. Fraenkel, Phys. Rev. C 24, 488 (1981).